Comparison of visible-near infrared and mid-infrared spectroscopy for classification of Huanglongbing and Citrus Canker infected leaves

Sindhuja Sankaran[1], Reza Ehsani[2*]

(1. *Department of Biological Systems Engineering, Washington State University, PO Box 646120, Pullman, WA 99163, USA*;
2. *Citrus Research and Education Center, University of Florida/IFAS, Lake Alfred, FL 33850, USA*)

Abstract: In this study, visible-near infrared spectroscopy and mid-infrared spectroscopy were compared to evaluate their applicability in classifying citrus leaves infected with canker and Huanglongbing (HLB) from healthy citrus leaves. The visible-near infrared spectra in the range 350-2,500 nm and mid-infrared spectra in the range of 5.15-10.72 μm were collected from healthy and diseased (canker, HLB) leaves. Following the spectral data collection, the data were preprocessed and classification was performed using two classifiers, quadratic discriminant analysis (QDA) and k-nearest neighbor (kNN). The classifiers (QDA, kNN) resulted in an average overall and individual class classification accuracy of about 90% or more. Mid-infrared spectroscopy provided high classification accuracy especially in identifying HLB-infected leaves; while, visible-near infrared spectroscopy was better suited for canker detection. Both methods have their own merits such as visible-near infrared spectroscopy offers non-invasive disease detection; while mid-infrared spectroscopy represents the chemical profile of the leaf, which may allow potential detection in asymptomatic stages.

Keywords: disease detection, classification, quadratic discriminant analysis, k-nearest neighbor

Citation: Sankaran, S., and R. Ehsani. 2013. Comparison of visible-near infrared and mid-infrared spectroscopy for classification of Huanglongbing and citrus canker infected leaves. Agric Eng Int: CIGR Journal, 15(3): 75−79.

1 Introduction

Citrus canker and Huanglongbing (HLB) are two major bacterial diseases in Florida affecting the yield and quality of citrus. The symptoms of these diseases depend on the age and severity of the infection. The leaf symptoms of HLB are chlorosis and blotchy mottle (Halbert and Manjunath, 2004; Gottwald, 2010), while, the canker symptoms are tiny, slightly raised blister-like lesions (Qin et al., 2009). Both these diseases lead to stem dieback, tree decline and eventually death of the citrus trees (Qin et al., 2009; Gottwald, 2010). Spectroscopic techniques offer rapid detection of citrus diseases. Changes in the plant physiological due to infection may affect the spectral signature that can be identified using optical sensors.

Several spectroscopic techniques such as visible-near infrared spectroscopy, mid-infrared spectroscopy, and fluorescence spectroscopy have been tested to identify their suitability in citrus disease detection (Belasque et al., 2008; Kim et al., 2009; Hawkins et al., 2010; Lins et al., 2009; Sankaran et al., 2010, 2011; Kumar et al., 2012). Although several of these studies have evaluated HLB and canker separately, there is no detailed study on spectroscopic techniques assessing both these diseases together. Therefore, the major objective of this work was to evaluate the performance of visible-near infrared spectroscopy and mid-infrared spectroscopy in classifying canker and HLB-infected leaves from healthy leaves concurrently.

Received date: 2013-03-12 **Accepted date:** 2013-07-29

*** Corresponding author: R. Ehsani,** Citrus Research and Education Center, University of Florida/IFAS, Lake Alfred, FL 33850, USA. Email: ehsani@ufl.edu, Phone: 1-863-956-8770, Fax: 1-863-956-4631.

2 Materials and methods

2.1 Spectrometers

A spectroradiometer (SVC HR-1024, Spectra Vista Cooperation, NY) was used to collect visible-near infrared spectra between 350 nm to 2,500 nm from the upper surface (adaxial surface) of the leaf. A field of view of 4° was used with an integration time of 4 ms. Similarly, mid-infrared spectra were acquired using a mid-infrared spectrometer (InfraSpec VFA-IR, Wilks Enterprise Inc., East Norwalk, CT) in the range 5.15 to 10.72 μm (1,942 to 933 cm^{-1}). Both the spectrometers are portable and applicable for field-based measurements. Figure 1 represents representative visible-near infrared and mid-infrared spectra.

2.2 Data Collection

Leaf samples were collected from healthy, HLB- and canker-infected citrus trees of Valencia cultivar located at the Citrus Research and Education Center (CREC) groves, Lake Alfred, FL. Each leaf sample set comprised of 4 to 5 leaves. The samples were collected from 30 healthy, 30 HLB- and 30 canker-infected trees. At first, visible-near infrared spectra were collected using the spectroradiometer placed at a distance of 0.5 m. Two 500 W portable halogen lamps were used as lighting source. Prior to the spectral data collection, a reference spectrum was acquired from a 25.4 × 25.1 cm white reference panel (Spectralon Reflectance Target, CSTM-SRT-99-100, Spectra Vista Cooperation, NY) using the spectroradiometer. The reference spectrum is a measure of 100% reflectance at each wavelength. The spectrum from the sample is adjusted based on the reference spectrum. Five spectra were collected from each sample set and averaged for analysis. The dataset was comprised of 90 spectra (30 sample sets × 3 groups). The data were collected under controlled laboratory conditions. Following the visible-near infrared spectral data collection, the leaf samples were processed for collecting the mid-infrared spectra as follows.

The leaves were ground into fine powder with a motor and pestle by adding some liquid nitrogen. The powdered leaves were placed on the crystal window of the mid-infrared spectrometer (InfraSpec VFA-IR spectrometer, Wilks Enterprises Inc., East Norwalk, CT), and spectra were collected using the IGOR Pro 6.01 program (WaveMetrics Inc., Portland, OR). The instrument was operated on attenuated total reflection mode and the baseline corrected absorbance spectra were saved for further processing. A scan time of 1 min was used. The spectrum collected from the crystal window in absence of a sample was used as a reference spectrum. A set of three spectra was acquired from each sample set. Two of the spectra were outliers. Therefore, the total number of spectral data was 268 (30 sample sets × 3 spectra × 3 groups).

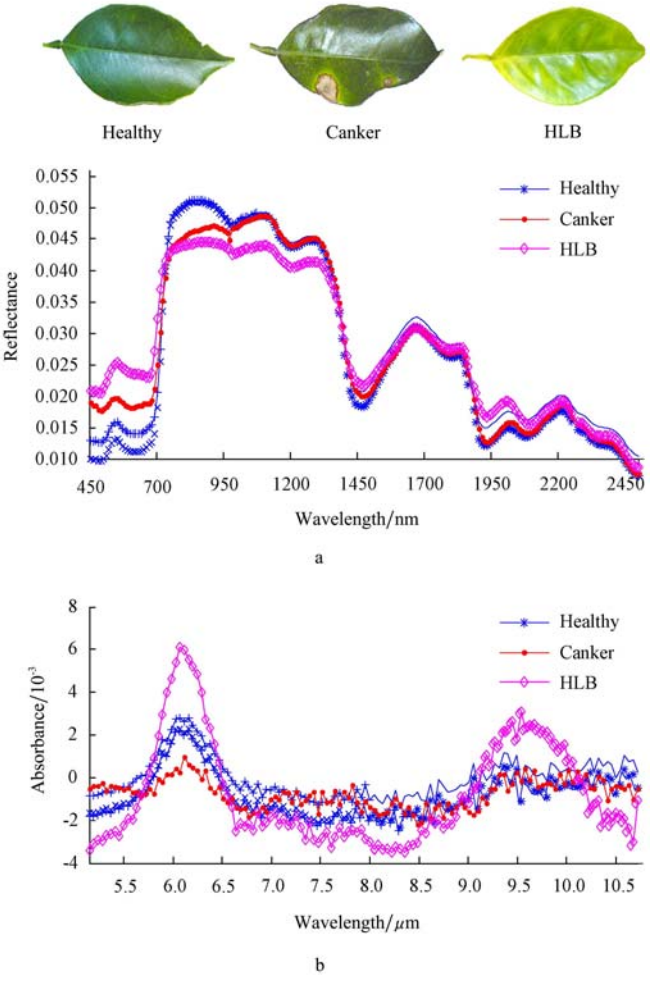

Figure 1 Leaf samples with representative visible-near infrared (a) and mid-infrared spectra (b)

2.2 Data analysis

The visible-near infrared and mid-infrared spectra were preprocessed prior to classification. Visible-infrared data were normalized and averaged every 10 nm to reduce the number of spectral features from 989 to 216. Similarly, the mid-infrared spectra were baseline corrected and the water spectra (5.15-6.73 μm) were

removed from the data, thereby reducing the number of features from 128 to 90 features. Principal component analysis (PCA) was performed to reduce the spectral features further into uncorrelated variables termed as principal components (PCs, Figure 2). PCs representing 96% variance within the data were used as input data to train the classifiers (3 for visible-infrared spectra, 7 for mid-infrared spectra). The PC scores were randomized, and 75% of data were used for training the classification algorithm, while 25% of data were used as test dataset. For the visible-near infrared data, the numbers of samples in the training and test datasets were 68 and 22, respectively. Similarly, the corresponding numbers for mid-infrared data were 201 and 67. Two classification algorithms, quadratic discriminant analysis (QDA) and k-nearest neighbor (kNN, k = 1) were used for classification. The algorithms were run three times and their performances were assessed based on the average classification accuracies (overall and individual class).

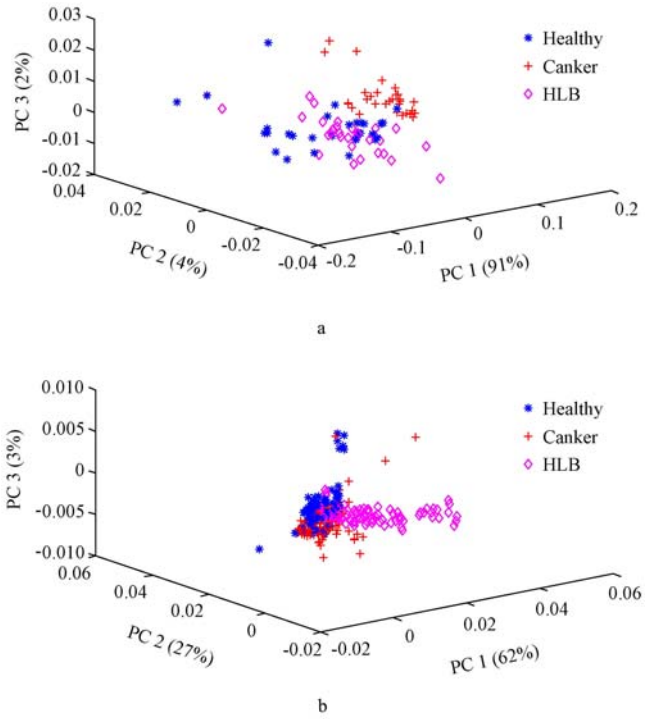

Figure 2 Principal component analysis plots for visible-near infrared (a) and mid-infrared (b) spectroscopy

3 Results and discussion

3.1 Visible-near infrared spectroscopy

Figure 1 represents the visible-near infrared spectra of healthy, canker-infected and HLB-infected leaves. The spectral reflectance pattern of healthy and diseased leaves showed a generalized pattern in the visible-near infrared region. The reflectance of healthy leaves is lower than diseased leaves in the visible region, while their reflectance is higher than those of diseased leaves in near infrared region. When the classification studies were performed using the visible-near infrared spectral data, it was found that the classification accuracies of QDA were better than the kNN (Table 1). The major difference in the performance of QDA and kNN-based classification was in average canker classification accuracies, where the QDA-based algorithm showed higher accuracy in identifying canker. Moreover, the average canker classification accuracy was also higher than those of HLB class classification accuracy.

Table 1 Classification accuracies (average ± standard deviation) acquired using QDA and kNN while classifying healthy, canker and HLB-infected leaves

Classifier	Healthy/%	Canker/%	HLB/%	Overall/%
Visible-near infrared spectroscopy				
Quadratic discriminant analysis	86.3 ± 1.0	100.0 ± 0.0	90.5 ± 16.5	92.5 ± 5.3
k-nearest neighbor	86.3 ± 1.0	90.5 ± 16.5	91.1 ± 7.8	89.4 ± 7.0
Mid-infrared spectroscopy				
Quadratic discriminant analysis	100.0 ± 0.0	97.0 ± 2.6	97.1 ± 2.5	98.0 ± 0.9
k-nearest neighbor	100.0 ± 0.0	97.0 ± 2.6	100.0 ± 0.0	99.0 ± 0.9

3.2 Mid-infrared spectroscopy

The mid-infrared spectra of the citrus leaves showed a distinct pattern, especially the HLB-infected leaves due to the starch accumulation as reported in literature (Sankaran et al., 2010). The kNN-based algorithm performed better resulting in higher average HLB class classification accuracy than those of QDA. The healthy and canker class classification accuracies were similar in both QDA and kNN. The high average overall classification accuracy of both algorithms indicates that mid-infrared spectroscopy has a good potential in plant disease detection.

3.3 Comparison of visible-near infrared and mid-infrared spectroscopy

Both the spectroscopic techniques resulted in average overall classification accuracies of about 90% and higher. The mid-infrared spectroscopy resulted in higher overall

and individual class classification accuracies (except canker) than visible-near infrared spectroscopy in most cases. The reason for this could be the working principle of the mid-infrared region, where the biochemical signature of the leaf is visible rather than the change in reflectance based on the plant physiology as estimated using visible-near infrared technique. Thus, the mid-infrared spectroscopy is capable of detecting biochemical compounds such as sugars and acids in leaves and other biological materials (Mascarenhas et al., 2000; Kačuráková, 2001; Aouidi et al., 2012). For example, the starch, which is known to accumulate in HLB-infected leaves, can be easily identified using mid-infrared spectroscopy as seen in Figure 1 (9-10.5 μm) (Dupuy et al., 1997; Mascarenhas et al., 2000; Sankaran et al., 2010). This is especially advantageous for detecting HLB-infected leaves as starch accumulation begins even before symptoms begin to appear. However, the major limitation of mid-infrared spectroscopy is the need for sample preparation by grinding the leaves into small particles. Considering this aspect, visible-near infrared spectroscopy is a rapid, non-destructive method, which does not require any sample processing. In this work, visible-near infrared spectroscopy was found to be better for identifying canker-infected leaves.

4 Conclusions

Both UV-visible spectroscopy and mid-infrared spectroscopy showed potential in classifying healthy and diseased leaves. Among the two methods, mid-infrared spectroscopy showed higher overall and HLB-class classification accuracies, while visible-near infrared spectroscopy showed better canker class classification accuracy. Some of the advantages of mid-infrared spectroscopy are that the method is not sensitive to changing light conditions and biochemical composition can be acquired using the spectral analysis. However, one of the major limitations is the need for sample processing. Visible-near infrared spectroscopy offers a direct, non-invasive method for diseased sample detection. Although, each of these spectroscopic methods has unique benefits, both visible-near infrared and mid-infrared spectroscopy could be applied for rapid evaluation of plant diseases in field conditions.

Acknowledgements

This research was funded by the Citrus Research and Development Foundation (CRDF) and the U.S. Department of Agriculture-National Institute of Food and Agriculture (USDA-NIFA). We would like thank Ms. Luba Polonik, Ms. Cindy Basnaw, Ms. Sherrie Buchanon, Ms. Shelley Jones and Dr. Jose Reyes for their help and support during this study.

References

Aouidi, F., N. Dupuy, J. Artaud, S. Roussas, M. Msallem, and I. P. Gaime. 2012. Rapid quantitative determination of oleuropein in olive leaves (*Olea europaea*) using mid-infrared spectroscopy combined with chemometric analyses. *Industrial Crops and Products,* 37(1): 292-297.

Belasque, Jr J., M. C. G. Gasparoto, and L.G. Marcassa. 2008. Detection of mechanical and disease stresses in citrus plants by fluorescence spectroscopy. *Applied Optics,* 47(11): 1922-1926.

Dupuy, N., C. Wojciechowski, C. D. Ta, J. P. Huvenne, and P. Legrand. 1997. Mid-infrared spectroscopy and chemometrics in corn starch classification. *Journal of Molecular Structure,* 401-411: 551-554.

Gottwald, T. R. 2010. Current epidemiological understanding of citrus Huanglongbing. *Annual Review of Phytopathology,* 48: 119-139.

Halbert, S. E., and K. L. Manjunath. 2004. Asian citrus psyllids (Sternorrhyncha: Psyllidae) and greening disease of citrus: a literature review and assessment of risk in Florida. *Florida Entomologist,* 87(3): 330-353.

Hawkins, S. A., B. Park, G. H. Poole, T. R. Gottwald, W. R. Windham, and K. C. Lawrence. 2010. Detection of Citrus Huanglongbing by Fourier Transform Infrared-Attenuated Total Reflection (FTIR-ATR) Spectroscopy. *Applied Spectroscopy,* 64: 100-103.

Kačuráková, M., and R. H. Wilson. 2001. Developments in

mid-infrared FT-IR spectroscopy of selected carbohydrates. *Carbohydrate Polymers,* 44(4): 291-303.

Kim, D. G., T. F. Burks, A. W. Schumann, M. Zekri, X. Zhao, and J. Qin. 2009. Detection of citrus greening using microscopic imaging. *Agricultural Engineering International: the CIGR Ejournal*, 11: manuscript No. 1194.

Kumar, A., W. S. Lee, R. Ehsani, G. Albrigo, C. Yang, and R. L. Mangan. 2012. Citrus greening disease detection using airborne multispectral and hyperspectral imaging. *Journal of Applied Remote sensing*, doi: 10.1117/1.JRS.6.063542 (accessedMay 5, 2012).

Lins, E., J. Belasque Jr, and L. G. Marcassa. 2009. Detection of citrus canker in citrus plants using laser induced fluorescence spectroscopy. *Precision Agriculture,* 10(4): 319-330.

Mascarenhas, M., J. Dighton, and G. A. Arbuckle. 2000. Characterization of plant carbohydrates and changes in leaf carbohydrate chemistry due to chemical and enzymatic degradation measured by microscopic ATR FT-IR spectroscopy. *Applied Spectroscopy,* 54(5): 681-686.

Qin, J., T. F. Burks, M. A. Ritenour, and W. G. Bonn. 2009. Detection of citrus canker using hyperspectral reflectance imaging with spectral information divergence. *Journal of Food Engineering,* 93(2): 183-191.

Sankaran, S., A. Mishra, J. M. Maja, and R. Ehsani. 2011. Visible-near infrared spectroscopy for detection of Huanglongbing in citrus orchards. *Computer and Electronics in Agriculture,* 77(2): 127-134.

Sankaran, S., R. Ehsani, and E. Etxeberria. 2010. Mid-infrared spectroscopy for detection of Huanglongbing (greening) in citrus leaves. *Talanta,* 83(2): 574-581.